

# PRESSURE AND HEAT LOAD IN A LHC TYPE CRYOGENIC VACUUM SYSTEM SUBJECTED TO ELECTRON CLOUD

V. Baglin, B. Jenninger, CERN, 1211 Geneva, Switzerland

## *Abstract*

The electron cloud is of major concern for most of the storage rings operating with large bunch currents and low bunch spacing. The Large Hadron Collider (LHC) operated at cryogenic temperature will have to face the electron cloud when running with proton beams. For this reason, the first experimental studies related to the electron cloud in a LHC type cryogenic vacuum system have been launched in 2002 after the closure of the Electron Positron Accumulator (EPA) synchrotron radiation experimental program. The cold bore experiment (COLDEX) has been installed in the CERN Super Proton Synchrotron (SPS) where electron clouds could be produced with proton beams. The detailed results of the investigations, which include measurements of the dynamic heat deposition, dynamic total pressure rise and residual gas composition as a function of beam operation dose will be presented. The beam conditioning efficiency is studied as a function of temperature. The results of dedicated experiments with pre-condensed gas layers onto the beam screen are shown. The preliminary results with 75 ns bunch spacing are presented. The experimental results obtained as a function of beam operation dose are compared to the outputs of the E-CLOUD simulation code. Finally, the implications to the LHC design and operation are discussed.

## INTRODUCTION

The Large Hadron Collider (LHC), presently under construction at CERN, will collide proton beams at 7 TeV. In each of the eight arcs of the machine, 23 regular FODO lattice cells of 106.92 m each, keep the particle on the closed orbit. The required magnetic dipole field and magnetic rigidity in the quadrupoles implies the use of the superconducting technology operating at 1.9 K [1]. In order to minimise the heat load induced by the beam onto the cryogenic system, a beam screen is inserted inside the vacuum cold bore held at 1.9 K. While absorbing the heat dissipated by the beam, the beam screen temperature increases along the half-cell cooling loop from 5 to 20 K. During the LHC operation, the beam vacuum is exposed to synchrotron radiation, electron and ion bombardment. This particle bombardment stimulates the desorption of gas molecules. Particularly, the hydrogen desorption

implies the perforation of  $\sim 4\%$  of the beam screen with slots in a way to provide an appropriate pumping towards the 1.9 K cold bore [2].

A limitation of the vacuum and the cryogenic systems is due to the beam induced electron cloud. The successive 1 ns short bunches of  $1.1 \times 10^{11}$  proton/bunch separated by 25 ns produce an electron cloud which builds up through a multipacting process. The native electrons coming from the residual gas ionisation and from the photoelectric effect are accelerated by the proton bunch potential. When impinging onto the beam screen, the electrons desorb gases, some of them are reflected and other create secondary electrons which in turn are accelerated by the next bunch. The secondary electron yield is a key parameter of the multipacting process. It is a characteristic of the vacuum chamber surface. The maximum amount of secondary electrons is defined by  $\delta_{\max}$  which is the maximum of the ratio of secondary electron produced (elastically reflected electron included) to the number of impinging electron. This maximum of the secondary electron yield curve occurs at a primary electron energy of  $\sim 250$  eV. In the "as received" state, when  $\delta_{\max} \sim 1.9$ , the simulations predict for the LHC an average arc heat load larger than 4 W/m with half of the nominal bunch current ( $0.5 \times 10^{11}$  proton/bunch) [3]. Since this heat load is not acceptable by the cryogenic system, a beam conditioning has been proposed to reduce the heat load to an acceptable value [4, 5]. Studies in the laboratory indicated that at room temperature and at cryogenic temperature, the  $\delta_{\max}$  could be reduced to  $\sim 1.1$  after electron bombardment [6, 7, 8]. In this case, according to the simulations, the average arc heat load with nominal bunch current reduces to  $\sim 0.2$  W/m [9]. To validate this beam conditioning scenario, there is a great interest to measure the reduction of the heat load due to the electron cloud in a LHC type vacuum chamber. Moreover, the potential effects onto the vacuum system due to the electron stimulated molecular desorption should be quantified to be able to predict and understand the LHC vacuum operation.

Perturbations attributed to an electron cloud onto some of the SPS pick-up were observed in 1998 [10]. In 1999, the first vacuum measurements with electron cloud distributed around the ring were performed [11, 12]. In 2002, the cold bore experiment (COLDEX) was installed in a bypass vacuum chamber of the SPS. This experiment is designed to simulate a LHC type cryogenic vacuum system. It was previously installed in a synchrotron radiation beam line of the Electron

Positron Accumulator (EPA) and into the EPA ring itself. It has been used intensively to study the photodesorption and the electron cloud issues onto a beam screen equipped with or without holes or with a cryosorber [13, 14, 15, 16].

The results obtained with COLDEX installed in the SPS during the run 2002 showed that there were large heat loads dissipated onto the beam screen and electron stimulated molecular desorption associated with electron clouds when the LHC type proton beams were circulating. Several studies, including a long term beam circulation, were performed. Although, a vacuum cleaning was observed, no significant reduction of the heat load dissipated onto the beam screen was observed [17]. For this reason and to test these results, a cold strip detector was designed and installed in 2003. Similarly to the previous COLDEX observations, unacceptable large heat load and a poor beam conditioning efficiency were reported after the run 2003 [18].

This paper presents in detail the results obtained with COLDEX during the SPS 2003 run. In section 2 a description of the COLDEX experimental set up is shown, COLDEX results are presented in section 3. They include measurements of the heat load and the partial pressure during a long term beam circulation, studies of beam conditioning at different temperatures, studies with condensed gas and studies with 75 ns bunch spacing. When applicable, the presented results are compared to previous measurements. In section 4, the benchmarking of the experimental results against the simulation results is discussed. Finally, in section 5, some important implications relative to the LHC design and operation are introduced.

## EXPERIMENTAL SET UP

A layout of the experimental set up is shown in Figure 1. The COLDEX experiment is made of a 2.2 m long OFE copper beam screen inserted into a 316 LN stainless steel cold bore. The inner diameter of the cold bore is 113 mm. The 67 mm inner diameter beam screen is perforated with 2 rows of rounded slots. The transparency is 1 %. The slots are of LHC type. A rounded slot is 2 mm wide and 7.5 mm long. Similarly to the LHC arc beam screen, an electron copper shield is mounted behind the slots. The role of the shield is to protect the cold bore from the electron cloud. The distance between the electron shield and the beam screen is  $\sim 4$  mm *i.e.* twice the LHC design. The beam screen and the cold bore temperatures can be controlled with a flow of gaseous helium and a liquid helium bath.

The COLDEX is installed inside a bypass vacuum chamber which can be move in and out of the beam

path. This tool allows to prepare an experiment and to control the dose received on a beam screen. After moving the COLDEX in the beam path, the two valves placed at the COLDEX extremities are opened and the experiment can start.

The pressure is measured upstream and downstream of COLDEX with calibrated Bayard-Alpert gauges. A calibrated residual gas analyser is located downstream to COLDEX. A vacuum port in the centre of COLDEX is equipped with a calibrated Bayard-Alpert gauge and a calibrated residual gas analyser. A room temperature chimney is placed at  $\sim 1$  mm from the beam screen vacuum port. A grid is installed in the beam screen vacuum port to shield the measurement port from the beam. The measurement of the pressure in the central port is expected to be an accurate representation of the desorbed molecules inside the beam screen. Before the experiment, the central Bayard-Alpert and residual gas analyser were baked to 300 °C. By thermal conduction, the chimney was baked to 160 °C. A bakeable electrode was installed inside the chimney to collect or repel the electrons which might have entered the vacuum measurement port.

The beam screen and the cold bore temperature are measured by calibrated temperature sensors (CERNOX). The helium flow along the beam screen is measured with a calibrated flow meter. The heat load dissipated onto the beam screen is determined from the two calibrated temperature sensors located upstream and downstream to the beam screen and the mass flow. A heater wire extended along the beam screen is used to check the calibration from the heat load measurement. Agreement within 20 % is found between the power dissipated by the wire due to the Joule effect and the measured heat load onto the beam screen. A heat load of 100 mW/m is found to be significantly measurable. Before and after to the experiments, the background was measured to be  $\sim 1.4$  W/m. This background is due to the thermal radiation coming from the extremities which are at room temperature.

The electron shield located behind the slots is made of several pieces of copper. One of these 17.85 cm long pieces is electrically isolated and the impinging electron current induced by the electron cloud can be measured. In this way, a measurement of the electron cloud activity inside the beam screen can be made. An average electron energy of the cloud can be estimated from the heat load and the electron activity measurements.

To minimise the impedance seen by the beam, a cold warm transition thermally anchored at 80 K and bridged by radio frequency fingers is installed at each extremity of COLDEX. The transition is a 0.1 mm thick stainless steel coated with 2  $\mu\text{m}$  of copper. The transition from the beam pipe of 100 mm inner diameter to the beam screen of 67 mm inner diameter is tapered with an angle of 45°. The 0.3 m long cold

warm transition acts as trap where most of the molecules desorbed at the extremities of COLDEX will be condensed. Therefore, the gas load onto the beam screen inside COLDEX due to the room temperature vacuum chambers located on each side of COLDEX is minimised.

The beam screen used during the experiment was recovered from previous studies when installed inside the EPA ring. The accumulated synchrotron radiation dose was estimated to be  $\sim 10^{23}$  photon/m *i.e.*  $\sim 1/10$  of one year with nominal LHC operation. The beam screen was then stored under air atmosphere for 3 years before UHV cleaning and its installation in the SPS.

During all the experiment described below, the cold bore was kept at 3 K, where all the gases with the exception of He have a negligible vapour pressure. The beam screen was operated at 12 K, except in section “beam conditioning at different temperatures” where it was temporarily operated at 50 K.

A room temperature calorimeter is installed downstream to COLDEX [19]. This calorimeter, WAMPAC 3, performs a direct measurement of the dissipated heat onto a copper liner. The copper liner is inserted into a stainless steel vacuum chamber. The liner is 67 mm inner diameter and 36 cm long. The temperature measurement is done via a series of thermocouples installed onto the liner and the vacuum chamber. After half an hour of constant heat dissipated onto the liner, an equilibrium temperature is reached. The equilibrium temperature is calibrated *in-situ* against a known heat input distributed along the liner by Joule effect. The dissipated heat onto the liner is deduced from the knowledge of the thermal resistance and the measurement of the equilibrium temperature. The relative accuracy of the measurement is less than 5 %.

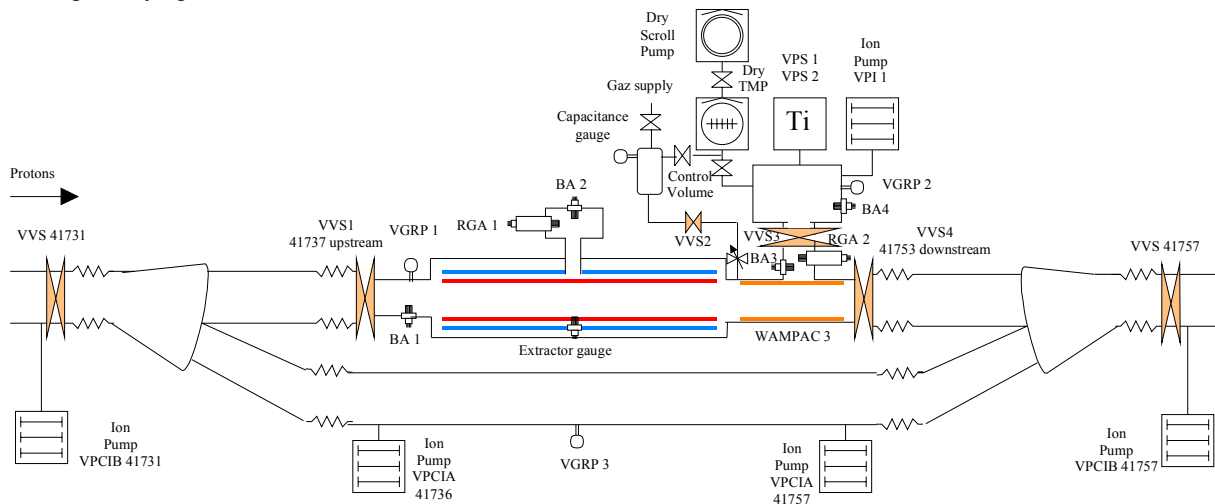


Figure 1 : Layout of the COLDEX experimental set up. VVS : vacuum valve, VGRP : Pirani- Penning gauge, RGA : residual gas analyser, BA : Bayard-Alpert gauge, VPCI : ion pump, VPS : Ti sublimation pump.

## RESULTS

During all the experiments described, the presence of an electron cloud in the SPS was also indicated by other SPS detectors such as the electron pick-ups, the pressure gauges, the strip detectors and the calorimeters. The SPS proton energy was set to 26 GeV in sections “long term circulation of a LHC type proton beam”, “beam conditioning at different temperatures” and “comparison with other detectors located in SPS”. In section “condensed gases and “operating with 75 ns bunch spacing”, the measurements were performed parasitically when a ramp of 450 GeV was applied in the SPS cycle. At 26 GeV, the bunch length is 2.8 ns and is 1.7 ns at 450 GeV. The bunch spacing was 25 ns, except in section 3.5 where it was 75 ns. Most of the time, the bunch current was  $1.1 \times 10^{11}$  protons/bunch.

### Long term circulation of a LHC type proton beam

#### Experimental preparation

After 2 months of pumping at room temperature with the valves located at the extremities closed, the COLDEX was evacuated to  $\sim 3 \times 10^{-7}$  Torr. The beam screen was cooled down first, before the cold bore. The system was held at cryogenic temperature for 12 days. The total pressures at the extremities were  $3 \times 10^{-10}$  and  $2 \times 10^{-9}$  Torr. The difference in the total pressures is due to the instrumentation’s outgassing located downstream of COLDEX. The total pressure in the centre of COLDEX was  $\sim 5 \times 10^{-10}$  Torr. The beam screen was then warmed-up to  $\sim 80$  K for a few hours (during which the total pressure increased to  $10^{-8}$  Torr)

before going back to 12 K. During this operation all the physisorbed gases onto the beam screen, with the exception of H<sub>2</sub>O, was flushed towards the cold bore. The H<sub>2</sub>O partial pressure upstream and downstream to COLDEX is estimated to be  $3 \times 10^{-10}$  and  $8 \times 10^{-10}$  Torr respectively. During 12 days, about  $2 \times 10^{19}$  H<sub>2</sub>O molecules could have been pumped at each COLDEX extremities. These H<sub>2</sub>O molecules were more likely pumped onto the  $\sim 0.5$  m long cold warm transitions thermally anchored at 80 K. So, the resulting amount of molecules condensed onto the beam screen is considered to be negligible and the beam screen surface before the experiment can be considered as a “bare” surface.

### Raw data

The experiment last about 8 days during which the LHC type proton beam was circulating through COLDEX. However, due to some operational difficulties, the beam parameters were not constant in time. The number of batches was varying from 1 to 4 with 72 bunches per batch. Each batch was separated by 225 ns. The bunch current was varying from  $\sim 0.7$  to  $1.4 \times 10^{11}$  proton/bunch. Finally, the duty cycle was varying from 10.5 to 98 %. As shown in Figure 2, these changes in the beam parameters and therefore in the electron cloud intensity itself, are reflected in the variations observed in the dynamic total pressure and the heat load dissipated onto the beam screen. Each data point is the average of 12 measurements over 2 minutes.

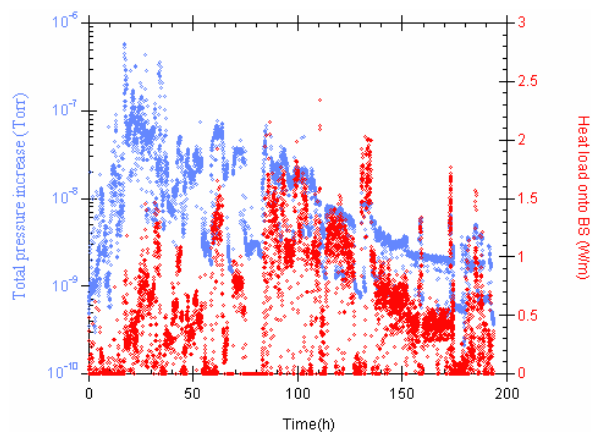


Figure 2 : Raw data of the dynamic pressure in COLDEX and the dissipated heat load onto the beam screen measured during the circulation of the LHC type proton beam in the SPS.

Obviously, the interpretation of such data is not trivial at all. To get comparable data sets, the current of each SPS cycle was integrated and an average current was computed. All the measured data were normalised to 4 batches with  $1.1 \times 10^{11}$  proton/bunch and 98 % duty cycle *i.e.* a SPS beam current of  $\sim 0.22$  A.

### Pressure increase

Figure 3 shows the result of the normalisation of the total pressure. It represents the expected measurements as if the SPS was always running with the same beam parameters.

The insert shows the evolution of the normalised total pressure increase during the first hours of beam operation. It is seen that after  $\sim 0.3$  A.h the normalised total pressure in the centre of COLDEX stops to increase and reaches a maximum value of  $\sim 5 \times 10^{-7}$  Torr. This phenomenon is due to the recycling effect of the physisorbed molecules *i.e.* the balance of the recycled molecules by the pumped molecules onto the beam screen. However, without normalisation, the maximum pressure increase measured in the experimental system is  $\sim 10^{-7}$  Torr (Figure 2). Therefore, in reality, the amount of desorbed gas is smaller than the amount suggested in Figure 3.

After an accumulated dose of 12 A.h, the dynamic pressure reduces to  $\sim 7 \times 10^{-9}$  Torr. A reduction of 2 orders of magnitude is observed. This vacuum cleaning is due to the bombardment of the cryogenic surface by the electrons of the cloud. This particle bombardment induces molecular desorption and surface changes.

The observations of the recycling phenomena and the vacuum cleaning are in agreement with experiments performed during the 2002 SPS run [17].

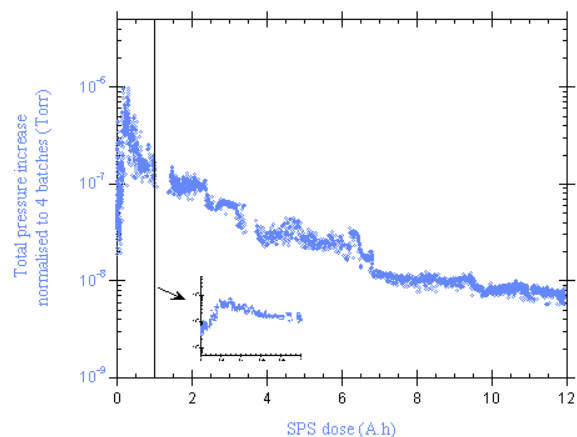


Figure 3 : Total pressure increase when an electron cloud is present in the COLDEX beam screen. The cold bore and the beam screen operate at 3 K and 12 K respectively. These data measured in the SPS are normalised to 4 batches with  $1.1 \times 10^{11}$  protons/bunch and 95 % duty cycle.

### Residual gas analysis

Figure 4 shows the normalised partial pressures increase as a function of the SPS dose. Since the base partial pressures before beam circulation were in the range  $10^{-11}$  to  $10^{-10}$  Torr, the electron cloud desorbs all the gas species shown here. At the start of the experiment, the gas composition is dominated by H<sub>2</sub>.

After 12 A.h accumulated, the  $H_2$  is decreased by about 2 orders of magnitude. At this point, a mixture of  $H_2$  and CO dominates the gas composition.

When a voltage from  $-1$  to  $1$  kV was applied on the central electrode, there were no significant changes in the total pressure or in the residual gas composition and there were no significant electron collection. So, the dynamic pressures increase of all the gases are thought to be relevant. Specially, the dynamic pressure of  $H_2O$  already observed during the 2002 SPS run but not shown, is included in Figure 4 [17].

During the experiment, an electron cloud is almost present everywhere in the SPS. Therefore, one can ask if the gas desorbed at the extremities of COLDEX perturb the measurement in the centre of COLDEX. A dedicated experiment performed with  $H_2$  injection showed that when a  $H_2$  pressure of  $10^{-6}$  Torr was applied at one extremity of COLDEX the pressure in the centre increased by less than  $10^{-10}$  Torr. Therefore, thanks to the pumping speed of the cold warm transition and the beam screen, the pressure measured in the centre of COLDEX is independent of the pressure at its extremities. However, with time, some gas desorbed from the room temperature part might be condensed onto the beam screen which in turn could perturb the pressure measurement in the centre and the heat load measurement. During the time of the experiment, the room temperature pressure at the extremities of COLDEX was comparable to the pressure in the centre of COLDEX. Assuming that all the desorbed gas at room temperature is condensed uniformly onto the beam screen, a rough estimation of the surface coverage indicates that a few monolayers of each gas species could be produced and condensed onto the beam screen. Nevertheless, due to the recycling effect, the surface coverage will stop to grow at a given equilibrium coverage. Given the recycling yields measured in 3.4, it can be shown that after 20 h of operation, the equilibrium surface coverage is a tenth of a monolayer. So, despite that some gas could be desorbed at room temperature and condensed onto the beam screen, the perturbations onto the pressure and the heat load measurements are expected to be negligible thanks to the recycling phenomena.

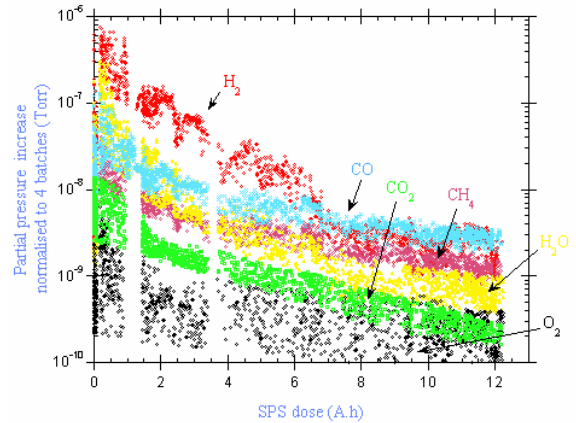


Figure 4 : Evolution with the SPS dose of the normalised dynamic partial pressure when a LHC type protons beam of 4 batches with  $1.1 \times 10^{11}$  protons/bunch is circulating through the COLDEX. The cold bore and beam screen operate at 3 K and 12 K respectively.

#### Electron activity inside the beam screen

An electron activity was measured with the electron shield collector when 4 batches of  $\sim 1.1 \times 10^{11}$  proton/bunch were circulating. In agreement with the appearance of an electron cloud in the COLDEX, this observation of an electron current is correlated with the pressure increase and the heat load dissipated onto the beam screen,

Taking into account the electron collection length, the beam screen transparency and assuming a uniform irradiation onto the beam screen by the cloud, an electron activity might be computed. From the heat load measurements on the beam screen and the electron activity measurements, the mean electron energy of the electron cloud might be derived

Figure 5 shows that the electron collection increases linearly when increasing the applied positive voltage onto the collector over 150 V. Therefore, we assume that at 150 V, the measured value correspond to the collector length of 0.179 m. It is seen that the measured current at 150 V decrease from 22  $\mu$ A after a dose of 0.25 A.h to 14  $\mu$ A after a dose of 12 A.h. This reduction of  $\sim 30\%$  is larger than the  $\sim 15\%$  heat load reduction observed after data analysis in Figure 6. This is in agreement with the retarding field detector data of another SPS experiment measuring the electron cloud energy distribution. This retarding field detector showed that the number of high energy electron was increasing while the electron activity was decreasing during the beam conditioning [20].

At a dose of 0.25 A.h, when 1.9 W/m is dissipated onto the beam screen, the calculated mean electron energy is 75 eV for an electron activity of 26 mA/m. At the end of the experimental period, at a dose of 12 A.h, when 1.6 W/m is dissipated onto the beam screen, the mean electron energy is 95 eV for an electron activity of 17 mA/m.



In the remaining part of the paper, it is assumed that the electron cloud in the COLDEX beam screen has a mean energy of 85 eV. If the collection length is over estimated by a factor 2, the mean electron energy would increase to 170 eV and the electron activity decrease to 10 mA/m. Consequently, an underestimation of the mean electron energy by a factor 2, will imply a subsequent over estimation of the desorption yield and the accumulated electron dose by a factor 2.

The electron cloud activity is observed in another detector such as the strip detector [18]. The collected intensity is 5 mA/m for a mean energy of 300 eV. This detector is operating in a dipole field mode and is located in a rectangular vacuum chamber (152 mm x 35.3 mm). It is not clear whether the difference with respect to the data presented in this paper could be attributed to the difference in geometry or the absence of the magnetic field. It should be emphasized that the electron cloud activity measured by the strip detector could not be reproduced by the simulation which predicts larger electron activity [21].

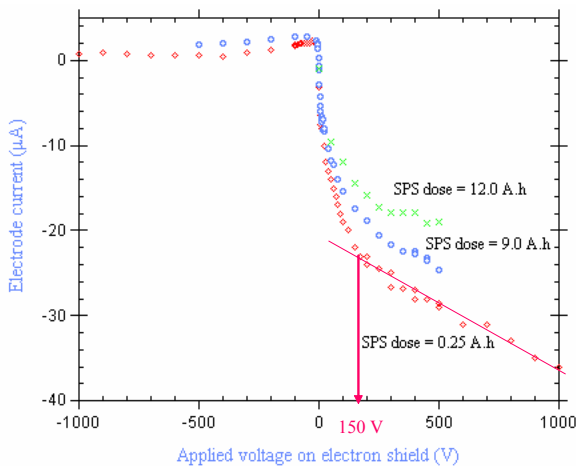


Figure 5 : Electron cloud activity measured on the electron shield collector located behind the beam screen slots as a function of the applied voltage.

### Dissipated heat load onto the beam screen

Figure 6 shows the dissipated heat load,  $HL$ , onto the beam screen in presence of an electron cloud. The raw data of Figure 2 were normalised to 4 batches with  $1.1 \times 10^{11}$  protons/bunch and 95 % duty cycle. For this reason, a scattering of the data is seen. With the dose, the heat load decreased from 1.9 W/m to 1.5 W/m after 12 A.h of operation in the SPS under electron cloud. In comparison with the pressure decrease of Figure 3 the beam conditioning rate is much less than the vacuum cleaning rate. These two processes are therefore not correlated in a simple manner.

The heat load data are fitted to an exponential decay. The fit is of the form  $HL = 1.9 e^{(-d/70)}$  where the  $d$  is the SPS dose. At first order, the beam conditioning rate is estimated to (0.02 +/- 0.001) W/m per A.h.

The electron cloud irradiates permanently the beam screen. The accumulated electron dose onto the beam screen is derived from the dissipated heat load and the mean electron energy. During the experiment, this dose is estimated to be 20 mC/mm<sup>2</sup>.

Thanks to the electron shield mounted behind the slots there was no significant heat loads onto the cold bore as compared to the 2002 run.

In agreement with previous observations, for a given bunch population, the dissipated heat load is proportional to the number of batches, from 1 to 4. This proportionality indicates that only a few bunches are required to trigger the electron cloud and therefore implies that the electron cloud is in equilibrium within a few bunches [17].

It should be stressed that the final dissipated heat load onto the beam screen at 12 K remains unchanged after a warm up to room temperature of the beam screen and the cold bore followed by a cool down to the operational temperature. So, the quantity of gas physisorbed onto the beam screen and accumulated during 12 A.h did not alter the level of the heat load dissipated onto the beam screen. Therefore, a limitation of the conditioning due to any parasitic outgassing located at the extremities of COLDEX or due to the outgassing of the beam screen itself seems improbable. The contrary means that a minor contribution of any outgassing area would strongly perturb the conditioning efficiency of a future machine.

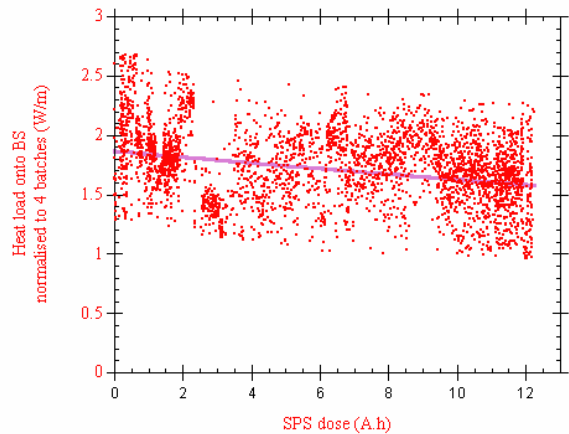


Figure 6 : Normalised dissipated power onto the beam screen due to the electron cloud as a function of the SPS dose. The cold bore and the beam screen operate at 3 K and 12 K respectively. These data measured in the SPS are normalised to 4 batches with  $1.1 \times 10^{11}$  protons/bunch and 95 % duty cycle. The data are fitted to an exponential decay.

On the other hand, thick layers of condensed gas as observed during the SPS 2002 run lead to a heat load dissipated onto the beam screen which rose to ~ 6 W/m after 90 h of operation (10 A.h) [17, 22]. However, initially, the dynamic pressure was ~  $10^{-6}$  Torr *i.e.* one order of magnitude larger than during the study presented here. Therefore, the gas desorbed, from the

as received elliptical beam screen and the unconditioned room temperature SPS vacuum chambers, and condensed onto the beam screen was larger in 2002 than the case shown in Figure 6. The resulting difference of thickness of condensed gas might explain the difference between the 2002 and 2003 results. Indeed, in 2002 after a warming up of the beam screen to remove the condensed gas, the heat load measured afterwards is in agreement with the data shown in Figure 6.

### Primary and recycling desorption yields

The electron stimulated molecular desorption yields are computed from the partial pressure increase and

from the electron flux,  $\dot{\Gamma}$ . The electron flux is deduced from the heat load measurements and the mean electron energy. The beam screen is assumed to be uniformly irradiated by the electrons of the cloud.

In a cryogenic beam vacuum system, one distinguishes two kinds of desorbed molecules which depend on the level of binding energies. The strongly bounded molecules are chemisorbed and their desorption is described by the primary desorption yield,  $\eta$ . The primary desorption is the source of gas into a vacuum chamber. The weakly bound molecules are physisorbed and their desorption is described by the recycling desorption yield,  $\eta'$ . This recycling yield characterises the ability of a physisorbed molecule on a cold surface to be desorbed (recycled) into the gas phase. The recycling yield is an increasing function of the gas coverage, so, in the absence of a perforated beam screen the pressure increases continuously. The recycling effect was demonstrated with  $H_2$  under synchrotron radiation bombardment [23, 13].

In a perforated beam screen and cold bore geometry, the recycling phenomena are usually manifested by a “slow” pressure increase within a few hours followed by an equilibrium value,  $\Delta P_{Eq}$ . When the flux of recycled gas is balanced by the flux of physisorbed gas onto the beam screen, the pressure equilibrates. The level is defined by the flux of gas stimulated by primary desorption over the pumping speed of the slots. So, the primary desorption yield is derived from equation (1) where  $G$  is a constant converting Torr.ℓ to molecules ( $3.2 \times 10^{19}$  molecules/(Torr.ℓ) at 300 K),  $C$  is the slots pumping speed.

$$\eta = \frac{G C \Delta P_{Eq}}{\dot{\Gamma}} \quad (1)$$

Figure 3 shows this slow dynamic pressure increase at the beginning of the run. The equilibrium pressure was reached at  $\sim 0.3$  A.h which correspond to  $\sim 20$  h of beam operation. Since the residual gas was dominated by  $H_2$ , this slow dynamic pressure increase is attributed to the  $H_2$  recycling. Therefore,  $H_2$  is in equilibrium and the primary desorption yield of  $H_2$  can be computed

using equation (1). Probably, the other gas species are not in equilibrium, then their primary desorption yield cannot be derived from these measurements.

Figure 7 shows the primary electron desorption yield of  $H_2$  as a function of electron dose in the case of a beam screen operating at 12 K. The yield initially equals  $\sim 10^{-1}$  and decrease to  $\sim 5 \times 10^{-4} H_2/e^-$  at a dose of  $2 \times 10^{19} e^-/cm^2$ . The total amount of desorbed molecules is given by integral of the curve, it equals  $\sim 100 \times 10^{15} H_2 \cdot cm^2$ . Also shown in Figure 7 is a fit of the data together with the fit parameters. The initial yield is in agreement with a previous measurement performed on an elliptical beam screen [17].

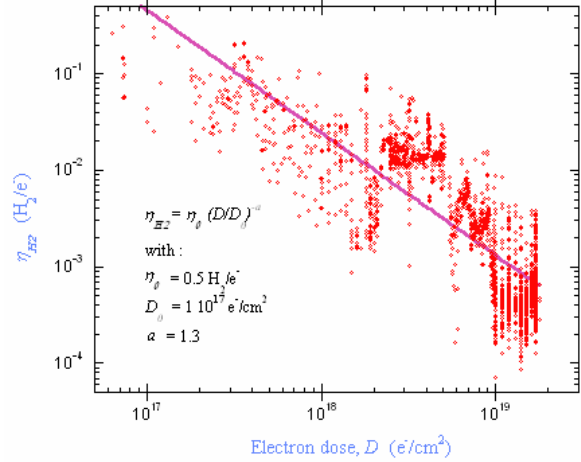


Figure 7 : Primary electron desorption yield of  $H_2$  as a function of electron dose. The copper beam screen operates at 12 K.

The sum of the primary and recycling desorption yield of all the gas species can be computed using equation (2) where  $S$  is the ideal pumping speed of the beam screen and  $\sigma$  is the sticking coefficient.

$$\frac{\eta + \eta'}{\sigma} = \frac{G C \Delta P}{\dot{\Gamma}} \quad (2)$$

Figure 8 shows the sum of the primary and recycling desorption yields over the sticking coefficient as a function of electron dose. The initial yields of  $H_2$ ,  $CH_4$ ,  $CO$  and  $CO_2$  are respectively  $10$ ,  $10^{-1}$ ,  $2 \times 10^{-1}$  and  $10^{-1}$ . These yields are in agreement with previous measurements [17]. During the exposure to the electron cloud, the yields decrease. This decrease is attributed to the vacuum cleaning *i.e.* the reduction with electron dose of the primary electron desorption yield.

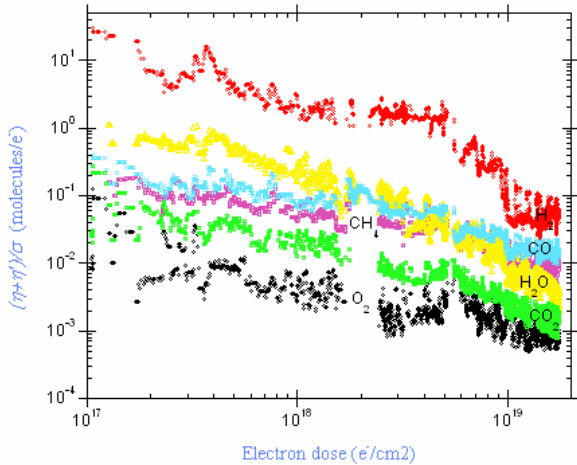


Figure 8 : Sum of the primary and recycling desorption yields over the sticking coefficient as a function of the electron dose when the beam screen operates at 12 K.

### Beam conditioning at different temperatures

During a dedicated experiment, care was taken to minimise the amount of physisorbed gas onto the beam screen. In the presence of an electron cloud, the beam screen temperature was varied from 10 to 50 K. In this temperature range, there was no variation of the heat load or of the beam conditioning rate.

This observation is in agreement with the comparison of the WAMPAC 3 data to the heat load dissipated onto the beam screen obtained during the long term circulation of a LHC type proton beam.

Figure 9 shows the raw data of the heat load dissipated onto the beam screen held at 12 K and the WAMPAC 3 held at room temperature. Clearly, there are no significant differences between 12 K and room temperature. Consequently, as far as there is no gas condensed onto the beam screen, the heat load dissipated by the electron cloud at 10-50 K and room temperature is similar. The conditioning rate is therefore almost temperature independent as already suggested by laboratory measurements [8].

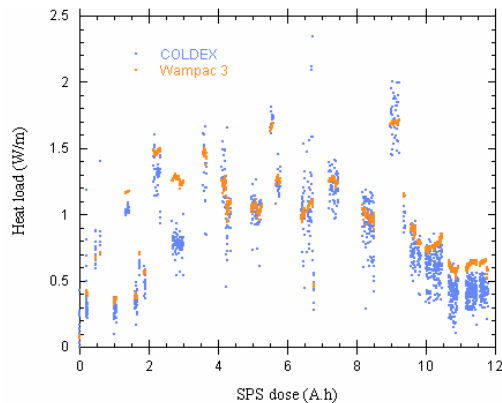


Figure 9 : Comparison of the heat load measured at room temperature and the heat load measured onto the beam screen held at 12 K.

### Comparison with other detectors located in the SPS

The behaviour as a function of the SPS dose of the above presented data is compared with other data of detectors located in the SPS. It includes a room temperature calorimeter, WAMPAC of inner diameter 140 mm and 1.3 m long [19], a room temperature pick-up calorimeter located in a rectangular vacuum chamber (152 mm x 35.3 mm) [24], a room temperature strip detector and a cryogenic strip detector installed in a rectangular vacuum chamber [18]. The two strip detectors operate most of the time in a dipole field mode and occasionally in a field free mode. The heat load deduced from the strip detectors, which measure the electron activity, is computed using the mean electron energy of the cloud as an input. To this goal, the strip detector itself and a retarding field detector are used. For the purpose of the comparison, all the data were normalised to 4 batches in the SPS (0.22 A) assuming proportionality of the electron cloud to the beam current.

After 2 A.h of SPS operation and up to 12 A.h, all the detectors, with the exception of the strip detector operating in a field free condition, exhibit a similar behaviour. The exception might be explained by the fact that the strip detector operates in two types of modes. In the SPS, a global decrease of the dissipated heat load from 25 to 30 mW/m per A.h is observed. This suggests that the beam conditioning rate is roughly independent of the geometry and / or the location of the detector. However, the level of the dissipated power in each detector varies from a few tens of mW/m to a few W/m. This span could be attributed to the different geometries between the detectors.

Despite the significant differences in the amount of dissipated power between the detectors, they all exhibit similar conditioning rate. Surprisingly, the amount of electrons available for conditioning does not seem to play a significant role. The possible explanation of this apparent discrepancy could lie in the different electron energy spectra within each detector location. Possibly, the electron cloud of the detectors which exhibit a large heat load are dominated by low energy electrons which do not contribute so efficiently to the beam conditioning. Consequently, as a rule of thumb, “small” vacuum chamber exhibit “large” heat load but are dominated by low energy electrons. On the other side, “large” vacuum chambers exhibit “small” heat load and are dominated by high energy electrons. The interplay of the level of heat load and the electron cloud energy spectra might explain why all the detectors exhibit a similar behaviour with the SPS beam dose.



## Condensed gases

During the operation of the LHC, some molecules could be physisorbed onto the beam screen in large quantities. Hence, there is great interest to study the effects onto the pressure and the heat load of condensed gases onto the beam screen. The studies with condensed gas were performed during dedicated period after a beam conditioning of more than 12 A.h. In this section, a compilation of new and old results is presented together [17]. More details are given in [22].

Before any of the experiment, with the valves closed, the gas is injected downstream to COLDEX. Since the beam screen is held at 12 K, all the gas is condensed at its extremity. So, the beam screen temperature is raised up to a value where the pressure along the beam screen equals a few  $10^{-6}$  Torr. Afterwards, the beam screen temperature is slowly decreased to 12 K while keeping the pressure along the beam screen uniform. The procedure was systematically applied in each experiment described below.

- The condensation of  $10^{15}$   $\text{H}_2/\text{cm}^2$  results in a significant recycling desorption while the electron cloud was present. The recycling yield is estimated to be  $3 \text{ H}_2/e^-$  for a sticking coefficient of 1. No significant increase of the dissipated heat load was observed [17].
- The condensation of  $5 \times 10^{15}$   $\text{CO}/\text{cm}^2$  results in a pressure increases due to the electron cloud. The recycling yield is estimated to be  $4 \times 10^{-1} \text{ CO}/e^-$  for a sticking coefficient of 1. No significant increase of the dissipated heat load was observed.
- The condensation of  $60 \times 10^{15}$   $\text{CO}/\text{cm}^2$  results in a large heat load up to 5 W/m when 1 batch was circulating. The heat load was associated with pressure spikes [17].
- The condensation of  $15 \times 10^{15}$   $\text{CO}_2/\text{cm}^2$  results in a pressure increases due to the electron cloud. The recycling yield is estimated to be  $1 \times 10^{-2} \text{ CO}_2/e^-$  for a sticking coefficient of 1. No significant increase of the dissipated heat load was observed. Under electron bombardment, a cracking of the  $\text{CO}_2$  into CO and  $\text{O}_2$  was noticed.

As discussed before, during the 2002 SPS run, the condensation of a thick layer of gas onto the beam screen is the source of a significant heat load. This condensed gas is presumably  $\text{H}_2\text{O}$  which originates from electron stimulated desorption of the room temperature part and cryogenic parts [17].

The above results indicate that the condensation of gas onto a cryogenic system plays an important role. Depending on the number of monolayers condensed and on the gas species, significant pressure increases and heat load appear when a machine operating at cryogenic temperature is submitted to an electron cloud.

## Operating with 75 ns bunch spacing

Since the electron cloud is a multipacting phenomenon, it requires that enough electrons remain in the vacuum chamber between successive bunches. If the distance between the bunches is increased, it is expected that the number of electron survivals is decreased. Therefore, the electron cloud activity shall be reduced when increasing the bunch distance. In LHC, during the first year of LHC operation, it is foreseen to operate with 75 ns bunch spacing instead of 25 ns. In order to explore this possibility, preliminary measurements have been performed in the SPS with the first 75 ns beams produced so far at CERN.

For this experiment, the cold bore was cooled down from room temperature to 3 K first while the beam screen was held at 230 K. After 2 days, the beam screen was cooled down to 12 K and the system was let for 4 days. Just before the start of the experiment, the valves located at the extremities were opened.

The beam circulating through COLDEX was made of 1 to 3 batches of 24 bunches each and  $1.1 \times 10^{11}$  protons/bunch. Thus, the beam current made of 3 batches with a bunch separation of 75 ns is equivalent to the beam current of 1 batch made with a bunch separation of 25 ns. When 3 batches were circulating no dissipated heat load onto the beam screen larger than 0.1 W/m nor pressure increase larger than  $2 \times 10^{-10}$  Torr were observed. However, this very encouraging result should be balanced by the room temperature observations. Indeed, in some of the room temperature vacuum chambers, pressure increases of a few  $10^{-9}$  Torr were measured while 2 and 3 batches were circulated. Nevertheless, the electron signal might be due to some proton trapped in the empty bucket. More studies are planned during the next SPS run in 2004 with 75 ns bunch separation.

## E-CLOUD CODE BENCHMARKING

The data presented in this paper have been crosschecked against the E-CLOUD code [25]. The parameters which are measured and predicted are compared against the simulated parameters. Table 1 shows the results of this comparison. In this table, the maximum of the secondary electron yield,  $\delta_{\text{max}}$ , is estimated following the secondary electron yield reduction curve by using the electron dose as an input [6]. All the data with an asterisk are predicted data from the measurements or the simulations.

The first column shows the experimental data. The heat load and the electron activity are directly measured. The mean energy of the cloud is deduced from the two above measurements (3.1.5). The combination of this mean energy and the dissipated

heat load allows to estimate the electron dose (3.1.6). The knowledge of the electron dose allows the estimation of  $\delta_{\max}$ .

The second column shows the simulated data [26]. For this simulation, the  $\delta_{\max}$  parameter is set to 1.3. The heat load, the electron activity, the mean energy, the fraction of electron above 30 eV are outputs of the code. Starting from a  $\delta_{\max} = 2$ , the combination of the simulated mean energy, the simulated fraction of electron having an energy above 30 eV and the heat load measured over the first two minutes, allows to estimate the electron dose received during the first two minutes. This electron dose is used to estimate a new  $\delta_{\max}$ . This value is used as an input to simulate a new mean energy and a new fraction of electron having an energy above 30 eV. In combination with the heat load measured over the next two minutes, a new dose is computed from which a new  $\delta_{\max}$  is estimated. This process is repeated several times up to the final heat load value.

The Table 1 shows that the measured and predicted data agree with the simulated data. So, the heat load observed in COLDEX and WAMPAC 3 during the 2003 SPS run is compatible with a  $\delta_{\max} \sim 1.2 - 1.3$ .

Table 1 : Comparison of the measured and the predicted parameters against the simulated parameters. The data with an asterisk are predicted data from the measurements or the simulations.

	Measurements	Simulation
Heat load (W/m)	1.6	1.6
Electron activity (mA/m)	17	21
Mean energy (eV)	85*	100
Fraction of electron above 30 eV	n.a.	~ 70 %
Electron dose (mC/mm <sup>2</sup> )	20*	10*
$\delta_{\max}$	1.1*	1.2*

## IMPLICATIONS FOR THE LHC

### *Beam conditioning during the scrubbing period*

In the LHC, at injection energy, the budget for electron cloud is set to 1.5 W/m and set to 1 W/m at collision energy [27]. To reach such a value, a beam conditioning will be required. This conditioning will exist only when an electron cloud is present in the vacuum chamber. It will be done during dedicated periods where the machine parameters can be adjusted to optimise the conditioning efficiency. This

conditioning shall be performed at injection energy where the heat load budget for the electron cloud is the largest.

A crude estimate of the LHC beam conditioning time can be done by a simple extrapolation of the SPS data. The rate derived from Figure 6 is assumed to be the same during the LHC conditioning time. Therefore any contributions due to bunch length, vacuum chamber dimensions, gas condensation onto the beam screen or others are not taken into account.

To extrapolate the data to the LHC, a normalisation should take into account the filling factor of the LHC and the number of batches,  $N$ , circulating in the SPS. Since it has been shown that the dissipated power remains linear with the number of circulating batches, the equivalent LHC power,  $H_{LHC}$ , is expressed in (3) as a function of the SPS power,  $H_{SPS}$ .

$$H_{LHC} = \frac{10.09}{N} H_{SPS} \quad (3)$$

Equation (3) shows that a power of 0.4 W/m with 4 batches in SPS (0.22 A) is equivalent to 1 W/m in LHC (0.56 A). From the fit given in 3.1.6, the dose required to reduce the power in the SPS to 0.4 W/m is estimated to be 100 A.h. This dose represents 20 days with 100 % efficiency operation with 4 batches. During this time, the amount of energy dissipated is 20 W/m.day.

Due to the larger beam current of the LHC, the required amount of energy to be dissipated would be 50 W/m.day. So, in the case that 1 W/m is permanently dissipated onto the LHC beam screen, about 50 days would be required to perform the beam conditioning.

It is stressed that these preliminary estimations have to be consolidated by further theoretical and experimental studies in the laboratory and in the SPS or in other machines. Particularly, some significant differences between the electron cloud in the SPS and the electron cloud in the LHC could originate from the vacuum chamber geometry, bunch parameters and bunch pattern. Non-linearities result from these differences. The outcome of a direct extrapolation of the SPS data to the LHC scale shall be taken with care.

The beam conditioning efficiency is optimised when using large bunch currents. In such a case, the high energy of the electrons in the cloud increases the efficiency of the beam conditioning. Adjustments of the beam filling pattern, introduction of 75 ns bunch spacing or satellite bunch or other means to clear / reduce the electron cloud shall be done to minimise the amount of dissipated heat load onto the beam screen. Appropriate cooling scheme shall be use to minimise the amount of condensed gas onto the beam screen.

### Lifetimes due to pressure increase during the scrubbing period

The electron cloud present in the LHC, will be associate to the electron stimulated molecular desorption. As a consequence, the pressure will rise inside the LHC vacuum chamber.

At injection energy (450 GeV), the proton beam experiences multiple Coulomb scattering on the residual gas. After several turns, this effect will increase the proton beam emittance. During the beam conditioning, an acceptable e-folding time is  $\sim 1$  h, whereas during physics run it should be increase to 15 - 20 h [28].

At nominal energy (7 TeV), the dominating process is the beam loss due to the nuclear scattering. The scattered protons will dissipate their energy into the cold mass of the magnet. Since this loss is proportional to the gas density, a maximum allowed gas density could be calculated to ensure a lifetime of 100 h. The

proton scattering onto the nucleus of the residual gas split into inelastic interactions (60% of the cross-section) and elastic ones (40%). In the latter case the scattered protons survive until they reach the collimator system. In the former case most of the secondary particles impact onto the cold masses along the first 12 m downstream of the interaction point [29]. So, the chosen 100 h lifetime due to nuclear scattering leads to a heat dissipation onto the cold masses of 22 mW/m/beam.

The first row of Table 2 gives the maximum allowable gas densities at 7 TeV assuming a single gas species with 100 h nuclear scattering lifetime. For a beam screen operating at 15 K, the second row gives the equivalent pressure measured at 300 K (applying thermal transpiration correction). The third row shows the corresponding e-folding time due to the multiple Coulomb scattering. In the case of a mixture of gas, the final lifetime is the inverse of the sum of the inverse individual lifetime.

Table 2 : Gas densities and room temperature (RT) equivalent pressure for single gas species with 100 h lifetime due to nuclear scattering at 7 TeV. Emittance e-folding time at 450 GeV for usual gas species present in UHV and expected in the LHC.

		H <sub>2</sub>	CH <sub>4</sub>	H <sub>2</sub> O	CO	O <sub>2</sub>	CO <sub>2</sub>
At 7 TeV, single gas with $\tau_{\text{nuclear}} \text{ (h)} = 100$ h beam screen = 15 K	m <sup>-3</sup>	9.8x10 <sup>14</sup>	1.6x10 <sup>14</sup>	1.6x10 <sup>14</sup>	1.1x10 <sup>14</sup>	9.9x10 <sup>13</sup>	7.0x10 <sup>13</sup>
	Torr (eq. RT)	6.8x10 <sup>-9</sup>	1.1x10 <sup>-9</sup>	1.1x10 <sup>-9</sup>	7.6x10 <sup>-10</sup>	6.9x10 <sup>-10</sup>	4.9x10 <sup>-10</sup>
At 450 GeV	$\tau_e \text{ (h)}$	13	7	9	7	6	4

The experimental data shown in 3.1.4 are used as an example to illustrate the possible vacuum performance at the start of LHC. The main challenges of the beam interactions with the vacuum system will be to minimise the radiation level, the background to the experiments, the coulomb scattering, the nuclear scattering and the deposited heat load on the beam screen.

Using the data shown in Figure 4 and Table 2, the 450 GeV e-folding time for each gas and the sum ( $\Sigma$ ) of all the gasses is computed as a function of proton dose in Figure 10. In this case, the power dissipated by the electron cloud was decreasing from 1.9 to 1.6 W/m (Figure 6). It is seen that after  $\sim 10$  A.h the value of 1 h is reached. This value is estimated to be enough to ensure a beam conditioning at 450 GeV with acceptable beams. So, at the start of the beam conditioning, the beam current should be reduced to increase the e-folding time accordingly. A beam conditioning during physics runs would require longer emittance growth time.

The dominant gas species in term of lifetime is CO. If the partial pressure of CO, in Figure 4, is due to the recycling, a warm up of the beam screen to shuffle the CO towards the cold bore will reduce the pressure and therefore increase the e-folding time. On the other hand, if this warm up does not increase the e-folding time, a

decrease of the dissipated power by the electron cloud would be required.

From these experimental data, it is estimated that an electron cloud dissipating 0.5, 1 and 1.5 W/m lead to 4, 2 and 1 h e-folding time. Thus, after 12 A.h in LHC at 450 GeV, a beam dissipating 0.5 W/m onto the beam screen might be ramped to 7 TeV.

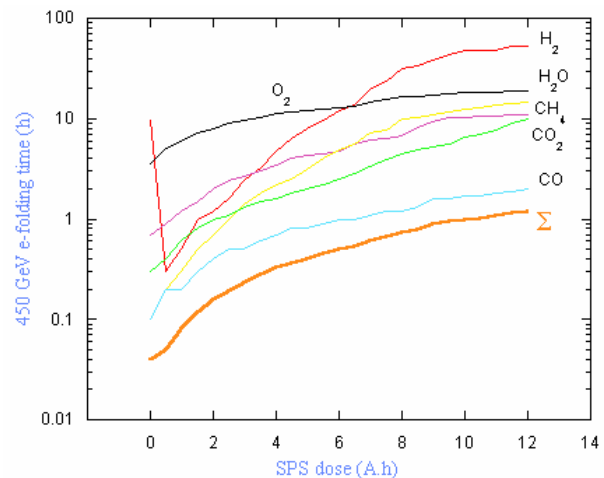


Figure 10 : 450 GeV e-folding time as a function of the SPS dose when 4 batches of LHC type beam are circulating in the SPS.

To estimate any potential limitations for beam conditioning at high energy, the nuclear lifetimes are computed. Figure 11 shows the computed 7 TeV nuclear lifetime in COLDEX when 4 batches of LHC type beams were circulated. The lifetime is dominated by CO. Therefore, after 12 A.h in LHC at 450 GeV, if one wants to perform a beam conditioning at 7 TeV the partial pressure of CO should be reduced. As stated before, there are two solutions : in the case this partial pressure is due to the recycling effect, a warm up of the beam screen would be sufficient, in the other case, a reduction of the beam current would be required. From these experimental data, it is estimated that an electron cloud dissipating 0.5, 1 and 1.5 W/m lead to 60, 30 and 20 h nuclear lifetime at 7 TeV.

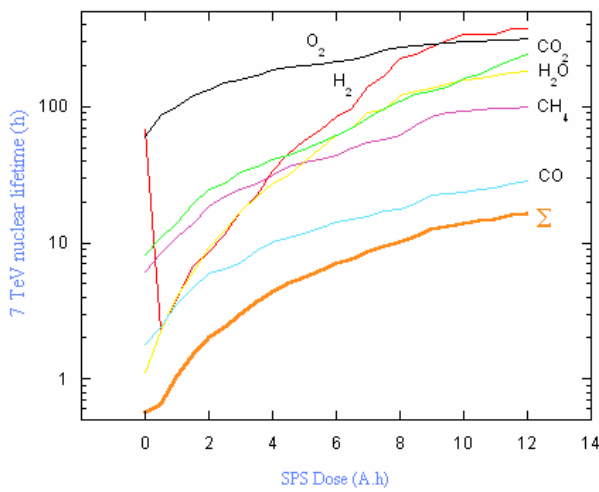


Figure 11 : 7 TeV nuclear lifetime as measured in the SPS when 4 batches of LHC type beams circulated through COLDEX.

### Condensed gases

During the operation of the LHC the primary desorbed gases will be condensed onto the beam screen and / or the cold bore and remain in the vacuum system until the vacuum system is warmed up. After the first year of the LHC operation with  $\sim 1/3$  of the nominal beam current *i.e.* only synchrotron radiation (no electron cloud), about  $6 \times 10^{15}$  CO/cm<sup>2</sup> and  $1 \times 10^{15}$  CO<sub>2</sub>/cm<sup>2</sup> would have been desorbed and condensed onto the beam screen [30]. Assuming a warming up and the end of the first year and taking into account the pre-conditioning due to the synchrotron radiation, it can be shown that still a few  $10^{15}$  molecules/cm<sup>2</sup> (defined here arbitrarily as a monolayer) can be desorbed. Therefore when switching to the beam conditioning regime or in the case of a quench or an uncontrolled cool down, a few monolayer of gas could be condensed onto the beam screen before the passage of the proton beam.

It has been shown that a few monolayers of condensed gases does not increase drastically the dissipated power by the electron cloud as compared to a “bare” surface but induce a significant pressure increase.

Figure 12 illustrates the possible consequences of a magnet quench [30]. It shows the simulated behaviour under electron stimulated molecular desorption of CO when  $25 \times 10^{15}$  CO/cm<sup>2</sup> are condensed locally over 2 m onto the beam screen. The mean energy of the electron cloud is assumed to be 100 eV. The recycling yield of CO is set to 4 CO/monolayer/e<sup>-</sup> [31].

When the dissipated energy of the electron cloud is 1.5 W/m, a strong pressure rise is observed. The level of the pressure exceeds the magnet quench limit for 1 h. To avoid the risk of quench, the beam current in the LHC could be reduced such that, say, 0.1 W/m is dissipated onto the beam screen. The local pressure reduces to  $4 \times 10^{-8}$  Torr for 20 h the required time for the beam to flush the gas from the beam screen towards the cold bore. During this period a significant proton scattering towards the magnet cold masses could be seen.

In some case, the reduction of the beam current might not be effective to achieve the required machine performances or might not be possible due to a too large irradiation of the machine elements. So, another method to flush the CO molecules towards the cold bore is required. This flushing is performed by a warming up of the beam screen with heaters located at the head of the BDS cooling circuit [32].

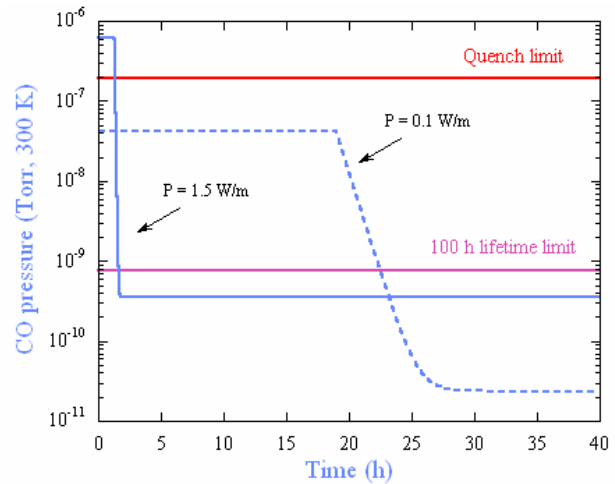


Figure 12 : Simulation of the CO partial pressure evolution in the LHC when  $25 \times 10^{15}$  CO/cm<sup>2</sup> condensed onto the beam screen is subjected to an electron cloud of 0.1 and 1.5 W/m.

## CONCLUSIONS

To predict and understand the vacuum behaviour during the LHC operation, a LHC type cryogenic vacuum chamber has been subjected to an electron cloud. The studies were performed with the 2m long COLDEX experiment installed in a field free region of the SPS while LHC type proton beams were circulated. These studies are the continuation of the previous experiments

performed in 2002 [17]. Direct measurements of total pressure, partial pressures and dissipated heat load onto the beam screen were performed under several conditions.

After about 8 days of run a dose of 12 A.h was accumulated. Since the dissipated power is linear with the beam current and due to the large variations of the SPS beam parameters, a normalisation of the raw data was necessary. The raw data were normalised to 0.22 A *i.e.* 40 % of the nominal LHC beam current.

At the end of the period, the total pressure decreased by 2 orders of magnitude and reached  $7 \times 10^{-9}$  Torr. During the same period, the dissipated power onto the beam screen decreased from 1.9 to 1.6 W/m. The electron activity measured by an electron collector located behind a beam screen slot indicated a similar behaviour. The estimated energy of the cloud is 85 eV. The accumulated electron dose onto the beam screen is estimated to be  $20 \text{ mC/mm}^2$ . As compared to the 2002 SPS run, the installation of electron shields located behind the beam screen slots was effective to reduce the heat load onto the cold bore to a negligible level [17].

The observations of the pressure increase and the heat load are in agreement with the previous data obtained with COLDEX in 2002 and more recent data [17, 18]. The conclusion is that in the SPS, a strong vacuum cleaning could be observed in a cryogenic vacuum chamber whereas a weak beam conditioning is observed. After a dose of 12 A.h, the level of the pressure is compatible with the LHC nominal operation whereas the amount of heat load limits the LHC to below nominal operation. Fortunately, the accumulated quantity of gas onto the beam screen during 12 A.h is shown not to be a limiting factor of the conditioning efficiency. Of course, since the contrary mean that a minor outgassing could hamper the conditioning efficiency of a cold surface which is not the case [8]. The large increase with time of the dissipated heat load observed in 2002 was not seen in the work presented here. This effect was due to the presence of a large amount of condensed gas, either  $\text{H}_2\text{O}$  or  $\text{CO}_2$ , onto the beam screen in the 2002 experiment [22].

During the long term beam circulation, the residual gas analysis showed that the main gas composition changed from  $\text{H}_2$  to a mixture of  $\text{H}_2$  and CO. Primary and recycling desorption yield to be used as input for vacuum simulations could be derived for the first time in a LHC type cryogenic vacuum chamber.

Finally, during the long term beam circulation experiment, the beam conditioning rate as a function of the temperature was studied. When no gas is condensed onto the beam screen surface, the rate is independent of the operating temperature in the range of 10 K to 300 K. The conditioning rate observed in COLDEX is similar to the rate observed in other detectors such as WAMPAC, the strip detectors and the pick up detector. The interplay of the electron energy spectra and the different vacuum chambers geometry could be the origin of such an observation.

The E-CLOUD code predictions are found to be in agreement with the experimental data presented here. However, the maximum secondary electron yield to be expected in COLDEX, which is predicted by the code, appears to be low close to 1.2-1.3, as compared to 1.5 for *in situ* secondary electron yield measurements performed in SPS [24]. Further investigations are required to validate this range of values.

Apart from the long term beam circulation experiment, several independent studies have been performed :

- The condensation of  $5 \times 10^{15} \text{ CO/cm}^2$  and  $15 \times 10^{15} \text{ CO}_2/\text{cm}^2$  have highlighted the recycling process. The recycling yield of these gases could be derived. But, contrary to the case of the thick layers of condensed CO ( $60 \times 10^{15} \text{ CO/cm}^2$ ) or  $\text{H}_2\text{O}$ , there are no significant heat load increase with respect to a bare surface after a beam conditioning of 12 A.h [17]. The implications to the LHC in the case of the condensation of CO after a quench have been discussed. The flushing of the CO towards the cold bore to limit the potential perturbations onto the beam operation provoked by overload of the cryogenic system or by irradiation of some machine element was proposed.
- The first 75 ns beams produced in the SPS were circulated through COLDEX. No heat load or pressure increase were observed. However, some pressure increase was noticed in other locations of the machine operating with room temperature vacuum chambers. This promising preliminary result shall be consolidated in the near future.

Assuming that 1 W/m could be dissipated onto the beam screen, estimations indicated that the energy required to perform the conditioning in the LHC is 50 (W/m).day. Therefore, the estimated time required to condition the LHC is 50 days. This preliminary estimation of the conditioning rate shall be consolidated in the future. For example, at this rate, assuming the SPS operation with 2 batches where very stable beams can circulates, 32 A.h shall be required to reduce the heat load from 1 W/m to 0.5 W/m. Nevertheless, significant differences between the gas composition, the vacuum chamber geometry, the beam parameters and the beam structure of the SPS and the LHC exist. There shall be differences in the development of the electron cloud in those two machines resulting from the different electron energy spectra. So, the results of a direct extrapolation of the SPS data to the LHC, particularly in terms of cleaning and beam conditioning rate, shall be taken with caution.

From the measurement of the residual gas composition, the estimation of the multiple Coulomb scattering lifetime at injection and nuclear scattering lifetime at collision energy have been made. Preliminary results show that after a beam conditioning of 12 A.h in LHC at 450 GeV, a proton beam dissipating 0.5 W/m onto the beam screen could be ramp to 7 TeV. In this case, the nuclear lifetime is estimated to be 60 h *i.e.* close to the required 100 h. To



the vacuum performance point of view, 7 TeV physics can be made below the electron cloud beam current threshold and maybe while conditioning the cryogenic vacuum chambers. Nevertheless, during operation, a careful monitoring of the vacuum and of the dissipated heat load shall be performed to minimise the level of induced radiation, the risks of quench and the overload of the cryogenic system.

The work presented in this paper demonstrates that a deep understanding of the electron cloud phenomena is required to control the radiation level, the background to the physics experiments, the beam emittance blow-up and the vacuum lifetime in the LHC. Further experiments are planned in 2004 to increase the understanding of a LHC type cryogenic vacuum system subjected to an electron cloud. Among others, the conditioning rate and the effects of condensed gases should be studied in details. Measurements in the laboratory with condensed gases under electron and photons bombardment are on the way. To assist the beam conditioning scenario, other possibilities to reduce the consequences of the electron cloud should be studied and validated in existing machines. Possible optimisation of the LHC filling pattern, implementation of satellite bunch or, when applicable, other means to clear the electron cloud (electrodes, solenoids) are good candidates.

## ACKNOWLEDGEMENTS

The authors would like to thank G. Arduini, P. Collier as well as the PS and SPS operating teams for running the PS and SPS machines with optimised beam quality. The support from S. Meunier and R. Wintzer, the SL vacuum team and M. Jimenez is acknowledged. The work carried out by N. Delruelle, O. Pirotte, Y. Drouyer, D. Legrand to refurbish and maintain the helium liquefier is gratefully acknowledged. The ECLoud simulations were kindly performed by D. Schulte and F. Zimmermann. Fruitful discussions with many colleagues of the Accelerator Physics and Vacuum Groups and particularly R. Cimino, O. Gröbner, N. Hilleret, J-M Laurent, D. Schulte and F. Zimmermann are acknowledged.

## REFERENCES

- [1] The LHC Study Group. The Large Hadron Collider, Conceptual Design, CERN/AC/95-05, CERN, Geneva, 1995.
- [2] Overview of the LHC Vacuum System, O. Gröbner. Vacuum 60 (2001) 25-34.
- [3] Electron-Cloud Effects in the LHC, F. Zimmermann. Proceedings of the ECLoud'02 workshop, CERN, Geneva, April 2002. CERN-2002-001.
- [4] Beam-Induced Electron Cloud in the LHC and Possible Remedies, V. Baglin, O. Brüning, R. Calder, F. Caspers, I.R. Collins, O. Gröbner, N. Hilleret, J-M. Laurent, M. Morvillo, M. Pivi, F. Ruggiero. Proceedings of the EPAC'98 Conference, Stockholm, June 1998. LHC Project Report 188, CERN, Geneva, June 1998.
- [5] Electron Cloud and Beam Scrubbing in the LHC, O. Brüning, F. Caspers, I.R. Collins, O. Gröbner, B. Henrist, N. Hilleret, J-M. Laurent, M. Morvillo, M. Pivi, F. Ruggiero, Zhang X. Proceedings of the PAC'99 Conference, New York, March 1999. CERN LHC Project Report 290, CERN, Geneva, April 1999.
- [6] Measurements at EPA of Vacuum and Electron-Cloud Related Effects, V. Baglin, I.R. Collins, O. Gröbner, C. Grünhagel, B. Henrist, N. Hilleret, B. Jenninger. Proceedings of the LHC workshop – Chamonix XI, Chamonix, January 2001. CERN-SL-2001-003 DI.
- [7] A Summary of Main Experimental Results Concerning the Secondary Electron Emission of Copper, V. Baglin, I.R. Collins, B. Henrist, N. Hilleret, G. Vorlauffer. CERN LHC Project Report 472, CERN, Geneva, August 2001.
- [8] Vacuum Chamber Surface electronic Properties Influencing Electron Cloud Phenomena, R. Cimino, I.R. Collins. LHC Project Report 669, CERN, Geneva, August 2003. Accepted for publication in Surface Science.
- [9] Electron Cloud : Operational Limitations and Simulations, F. Zimmermann. Proceedings of the LHC Performance workshop – Chamonix XII, Chamonix, March 2003. CERN-AB-2003-008 ADM.
- [10] Observations of the Electron Cloud Effect on Pick-Up Signals in the SPS, W. Hofle. Proceedings of the SPS & LEP Performance workshop – Chamonix X, Chamonix, January 2000. CERN-SL-2000-007 DI.
- [11] Observations in the SPS : Beam Emittance, Instabilities, G. Arduini. Proceedings of the SPS & LEP Performance workshop – Chamonix X, Chamonix, January 2000. CERN-SL-2000-007 DI.
- [12] Electron Cloud : SPS Vacuum Observations with LHC Type Beams, G. Arduini, K. Cornelis, M. Jimenez, G. Moulard, M. Pivi, K. Weiss. Proceedings of the SPS & LEP Performance workshop – Chamonix X, Chamonix, January 2000. CERN-SL-2000-007 DI.
- [13] First Results from COLDEX Applicable to the LHC Cryogenic Vacuum System, V. Baglin, I.R. Collins, C. Grünhagel, O. Gröbner, B. Jenninger. Proceedings of the EPAC'00 Conference, Vienna, June 2000. LHC Project Report 435, CERN, Geneva, September 2000.
- [14] Molecular Desorption by Synchrotron Radiation and Sticking Coefficient at Cryogenic Temperatures for H<sub>2</sub>, CH<sub>4</sub>, CO and CO<sub>2</sub>, V. Baglin, I.R. Collins, C. Grünhagel, O. Gröbner, B. Jenninger. Vacuum 67 (2002) 421-428.
- [15] Synchrotron Radiation Studies of the LHC Dipole beam Screen with COLDEX, V. Baglin, I.R. Collins, C. Grünhagel, O. Gröbner, B. Jenninger. Proceedings of the EPAC'02 Conference, Paris, June 2002. LHC Project Report 584, CERN, Geneva, July 2002.
- [16] Cryosorbers Studies For the LHC long Straight Section Beam Screens with COLDEX, V. Baglin, I.R. Collins, C. Grünhagel, O. Gröbner, B. Jenninger. Proceedings of the EPAC'02 Conference, Paris, June 2002. LHC Project Report 580, CERN, Geneva, July 2002.
- [17] Performance of a Cryogenic Vacuum System (COLDEX) with a LHC Type Proton Beam, V. Baglin, I.R. Collins, B. Jenninger. Vacuum 73 (2004) 201-206.
- [18] Electron Cloud Heat Load Estimations for the LHC Using Strip and retarding Field Detectors, J.M. Jimenez, B. Henrist, J-M Laurent, K. Weiss. LHC Project Report 677, CERN, Geneva, October 2003.
- [19] CERN SPS Electron Cloud Heat Load Measurements and Simulations. V. Baglin, B. Jenninger. Phys. Rev. ST. Accel. Beams 6, 063201 (2003).
- [20] Electron Cloud Energy and Power Measurement in SPS, J-M. Laurent, H. Song. CERN Vacuum Technical Note TN-04-02, CERN, Geneva, January 2004.
- [21] Electron Cloud Simulation Build Up with ECLoud, D. Schulte. Proceedings of the 31st ICFA Advanced Beam Dynamics

Workshop on Electron-Cloud Effects "E-CLOUD'04", Napa, California, April 19-23, 2004.

- [22] Gas Condensates onto a LHC Type Cryogenic Vacuum System Subjected to Electron Cloud. V. Baglin, B. Jenninger. Proceedings of the EPAC'04 Conference, Luzern, July 2004.
- [23] Investigation of Synchrotron Radiation-Induced Photodesorption in a Cryosorbing Quasiclosed Geometry, V.V. Anashin, O.B. Malyshev, V.N. Osipov, I.L. Maslennikov, W. C. Turner. J. Vac. Sci. Technol. A 12(5), Sep/Oct 1994, 2917-2921.
- [24] SEY & Pickup Calorimeter Measurements, N. Hilleret. Mini Workshop on SPS Scrubbing Run Results and Implications to the LHC, CERN, Geneva, 28<sup>th</sup> June 2002.
- [25] Practical User Guide for E-CLOUD, G. Rumolo, F. Zimmermann. CERN-SL-Note 2002-016 (AP), CERN, Geneva, November 2003.
- [26] Private communication, March 2004. Courtesy of D. Schulte and F. Zimmermann.
- [27] Tuning the Cryogenic System to the Machine, U. Wagner. Proceedings of the LHC Project Workshop - Chamonix XIII, CERN, Geneva, February 2004. CERN-AB-2004-014 ADM.
- [28] F. Ruggiero, private communication.
- [29] Momentum losses and momentum collimation in LHC: a first approach. B. Jeanneret. CERN SL/92-44 (EA), LHC Note 211, CERN, Geneva, 1992.
- [30] Running In – Commissioning with Beam, V. Baglin. Proceedings of the LHC workshop - Chamonix XII, CERN, Geneva, March 2003. CERN-AB-2003-008 ADM.
- [31] Measurements of the CO recycling yield at 100 eV, N. Hilleret, H. Tratnik. Private communication, 23/10/03.
- [32] Vacuum Transient during LHC Operation, V. Baglin. Proceedings of the LHC Project Workshop - Chamonix XIII, CERN, Geneva, February 2004. CERN-AB-2004-014 ADM.